Local Heat Flux Measurement in a Permanent Magnet Motor at No Load

Hanne K. Jussila, Andrey V. Mityakov, Sergey Z. Sapozhnikov,
Vladimir Y. Mityakov, and Juha Pyrhönen, *Member, IEEE*

Abstract—Heat transfer is a limiting factor in the performance of electrical machines. Measuring the heat flux in an electrical machine is traditionally carried out indirectly with temperature measurements as there are only a few sensors for heat flux measurements. This paper describes a new experimental method to measure the local heat flux inside an electrical machine. The measurement was proven successful in the air gap of the permanent magnet machine, 37 kW 2400 min^{-1}, under an influence of the air gap magnetic flux. The heat flux was measured by using sensors based on the transverse Seebeck effect. The test machine was an axial flux permanent magnet machine with two stator stacks and one internal, ironless rotor disc. A gradient heat flux sensor was installed in the air gap on the stator side. Local Nusselt and Reynolds numbers were calculated according to the measured heat flux results and compared with the results given by traditional methods to verify the new measurement method.

Index Terms—Axial flux permanent magnet (AFPM) machine, concentrated tooth winding, heat flux, heat flux measurement, permanent magnet machine.

NOMENCLATURE

A	Area [m^2]
B_{r}	Remanent flux density [T]
$D_{\mathrm{i,axial}}$	Internal diameter of the stator stack [m]
$D_{\mathrm{o,axial}}$	External diameter of the stator stack [m]
E	Electric field [V/m], thermo-electromotive force [V]
e	Thermo-electromotive force (emf) [V]
h	Heat transfer coefficient [W/(m^{2}K)]
h_{PM}	Thickness of permanent magnet [m]
h_{ys}	Stator yoke height [m]
I_{s}	Rated current [A]
k	Air thermal conductivity [W/(mK)]
k_{w5}	Winding factor of the fifth harmonic of the stator
m_{PM}	Mass of magnets [kg]
N_{s}	Winding turns in series per stator winding
Nu	Nusselt number
n_{s}	Speed [min^{-1}]
P	Pressure [Pa]
P_{out}	Output power [W]
p	Number of rotor poles
Q	Heat flux [W/m^2]
Q_{s}	Number of stator slots
q	Heat flux [W/m^2]
Re	Reynolds number
r	Radius [m]
S_0	Sensitivity [V/W]
T	Temperature [K, ^{o}C]
T_{N}	Rated torque [Nm]
U	Voltage [V]
δ	Length of air gap [m]
μ	Dynamic viscosity of the fluid [kg/(ms)]
ν	Kinematic air viscosity [m^2/s]
ρ	Density of the fluid [kg/m^3]
ρ_{PM}	Permanent magnet resistivity [$\mu\Omega$cm]
τ	Time variable [s]
ω	Rotor speed [s^{-1}].

I. INTRODUCTION

HEAT TRANSFER in electrical machines is one of the most challenging issues to be analyzed accurately. It is, however, one of the important limiting factors in the design of electrical machines [1], [2]. According to Howey *et al.* [3], "Accurate thermal analysis of axial flux permanent magnet (AFPM) machines is crucial in predicting maximum power output. Stator convective heat transfer is one of the most important and least investigated heat transfer mechanisms." So far, there have been only a few sensors available for direct heat flux measurements [4], and only temperature measurements have been possible. Nevertheless, they give only indirect information of the heat flux. Direct heat flux measurement in an electrical machine development offers a new useful tool for the designers.

In the world ever more concerned with saving energy and increasing efficiency, studying the thermal properties of machines has become an increasingly growing field of interest [5], [6]. An accurate estimation of the thermal behavior of an electrical machine is important considering the fact that safe operating conditions and overloading capabilities are dependent on the temperature rise [7]. Because of a number of variable factors involved, such as unknown loss contributions with their complicated 3-D distributions, it is obvious that exact determination of the thermal behavior of a machine is, in practice, very difficult [8], [9].

A very comprehensive literature review of the rotor-stator heat transfer and disc type electrical machines is presented by Howey *et al.* [10]. They have also extensively reviewed experimental techniques for convective heat transfer measurement.

Howey *et al.* [11] measured the stator convective heat transfer in a rotor-stator system. They used film heaters and also measured the temperature. Harmand *et al.* [12] measured the temperature of the rotor by infrared thermography. Further, they measured the mean flow fields using a double-pulsed laser technique. The heat transfer coefficient is calculated from the conductivity equation. In addition, in [13], the main difference compared with the present work is that in our case, the heat flux measurement is made in an actual AFPM machine, while Lim *et al.* made their tests in a large-scale rig, where silicone heater mats generate the heat. In this new heat flux measurement project, the purpose is to measure the local heat flux directly using gradient heat flux sensors (GHFS). The GHFS have been under study and development for a long time [14], but have not been used before in the air gap of an electrical machine.

In Section V, the local Nusselt number calculated according to the measured heat flux is compared with results obtained in other studies [11], [12].

In this paper, the local heat flux in a permanent magnet synchronous machine was measured using a GHFS. Developing such a method to a level where the measurement results are always reliable makes an improvement in the electrical machine development.

II. HFS

The GHFS are based on the transverse Seebeck effect, in which the thermo-electromotive force (thermo-emf) is proportional to the temperature gradient in the surface layer of bismuth. The Seebeck effect is the conversion of temperature differences directly into electricity [15]. GHFS allows measuring the local heat flux of any nature and practically for any objects of all forms without time delay.

The tests showed that the response time of the GHFS is about $10^{-8} - 10^{-9}$ s. Among the advantages of the GHFS are their small dimensions (from $1 \times 1 \times 0.1$ mm^3). Moreover, the high sensitivity (2–50 mV/W) of the GHFS allows their use without amplifiers, and their low resistance (1–10 Ω) provides the noise immunity of the measurement circuit.

In the current paper (for the first time in a PM motor), the GHFS made of anisotropic thermoelements (AT) were used. A construction and applications of the GHFS are described in [16]. The upper temperature limit for the sensors made of bismuth is limited by its melting point (541 K).

Commercially available sensors [4], which are made of a number of thermocouples, are connected differentially on both sides of the material with a known thermal conductivity. Sensors of this kind generate a thermo-emf proportional to the heat flux passing through the sensor. Instead, the sensors introduced here are made of an anisotropic material and have no thermocouple at all.

That is why the sensitivity of the proposed sensor is independent of the thickness in contrast to thermocouple sensors, which should be thick to reach a high sensitivity, which, again,
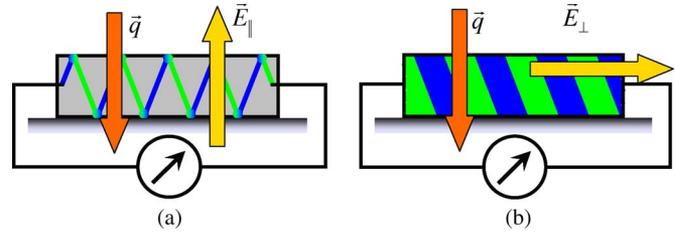

Fig. 1. (a) Thermocouple and (b) anisotropic HFS.

increases the response time. This conflict between sensitivity and response time is a fundamental and irrevocable characteristic of thermocouple sensors.

A. GHFS

There are only a few types of HFS available worldwide that are useful for research. In this case, the auxiliary-wall-type HFS are used, which represent flat plates, and are, because of their smaller dimensions, located normal to isothermal surfaces [17]. HFSs generate electric signals related to the average heat flux passing through the sensor.

A majority of the known HFSs are made of materials, the upper temperature level of which is about 300–500 K. Therefore, these sensors cannot be used for high-temperature measurements in power engineering, aircraft industry, metallurgy, and the like. The selection of natural materials suitable for new HFSs is limited. By using sliced composites as artificial AT (manufactured of metals, alloys, or semiconductors), it is possible to introduce a new generation of HFSs.

At present, auxiliary-wall-type HFSs are constructed of plates with differential thermocouple junctions inserted at their surfaces. Such a thermocouple can be a two-junction one, but more often, it is made as a battery of multiple thermoelectric junctions, where tens, hundreds, and sometimes even thousands of thermoelectric junctions are connected in series [Fig. 1(a)].

In thermocouple HFSs, the heat flux $\vec{q}$ [W/m^2] and the field of electric vectors $\vec{E}_\parallel$ [V/m] are parallel.

However, there are different HFSs based on AT [Fig. 1(b)], made of materials with anisotropy of thermal conductivity, electric conductivity, and thermo-emf. Because of anisotropy, in the sensors, the temperature gradients are produced in two directions: along and across the applied heat flux. This effect is known as transverse Seebeck effect. The electric field vector $\vec{E}_\perp$ is proportional to the transverse temperature gradient and is normal to the applied heat flux vector $\vec{q}$.

Because the sensors generate an output signal proportional to the transverse temperature gradient, which is proportional to the parallel temperature gradient, which in turn is proportional to the applied heat flux, the sensors are called "GHFS" in this paper.

There are few natural anisotropic materials that can be used as thermoelements, for example bismuth single crystals. Such a thermoelectric anisotropy can also be obtained by artificially produced tilted layered materials. A multilayer structure made of metals, alloys, and semiconductors can be also used as an HFS.

For HFSs based on artificial AT, it was shown that in transient thermal conditions, an electric signal is generated in a very thin
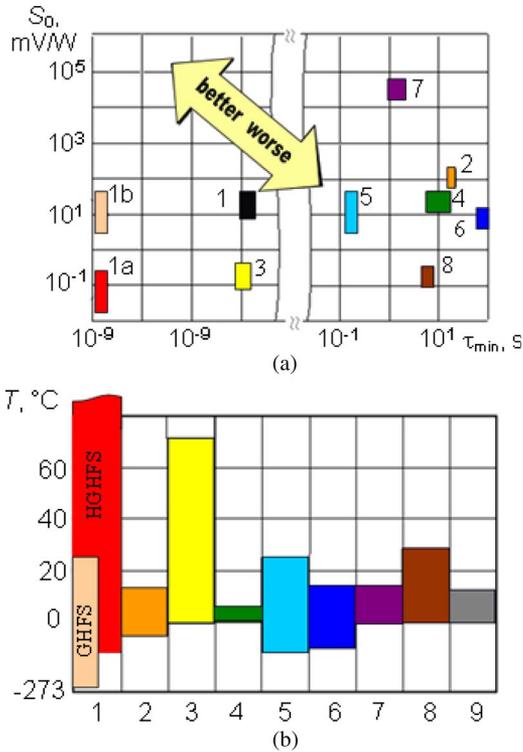
Fig. 2. Comparison of modern heat flux sensors by the (a) sensitivity S_0 and the response time $\tau_{\min}$ and (b) the temperature limit: 1—GHFS based on bismuth (1a) and HGHFS (1b); 2—Academy of Science (Ukraine); 3—Vatell (USA); 4—Wuntronic (Germany); 5—Captec (France); 6—Hukseflux (the Netherlands); 7—Laboratory of Physical Electronics (Switzerland); 8—Newport (USA); 9—TNO (the Netherlands) (no data of τ min); 10—ALTP FORTECH HTS GmbH (Germany) (no data of the operating temperature).

surface layer of the sensor resulting in a very small response time of sensors in the range of $10^{-8} - 10^{-9}$ s. The comparison of different sensors is presented in Fig. 2.

Many sensors have a sensitivity of the order of 10 mV/W and a response time of about 10 s. The temperature limit for most sensors is about 200 °C, the maximum temperature being 700 °C. In the present project, the sensors have a sensitivity 0, 1–10 mV/W with a response time of about 10 ns and the upper temperature limit of about 1000 °C.

The thermo-emf e_x of GHFS is proportional to the heat flux density q_Z, the sensor area A, and the sensitivity S_0:

$$e_x = q_z \cdot A \cdot S_0. \tag{1}$$

A GHFS design is shown in Fig. 3. Usually, a GHFS is a battery of a number of thermoelements 1 connected with a switch of polarity. The sizes of the battery in a plane are from 1×1 mm up to 10×10 mm and more, and the thickness is now reduced to 0.15 mm (which is close to the technologically accessible minimum).

In our experience, the GHFS had $S_0 = 5.12$ mV/W. The linearity of the function S_0 has an error no more than 5% in all temperature ranges. The GHFS signal does not depend on pressure. According to the tests, at least up to 30 MPa, the pressure has no significant impact on the sensor sensitivity. When a sensor is inserted in a travelling magnetic flux wave, some AC voltage will inevitably be induced in the sensor. In addition, a significant amount of noise can be induced in it.
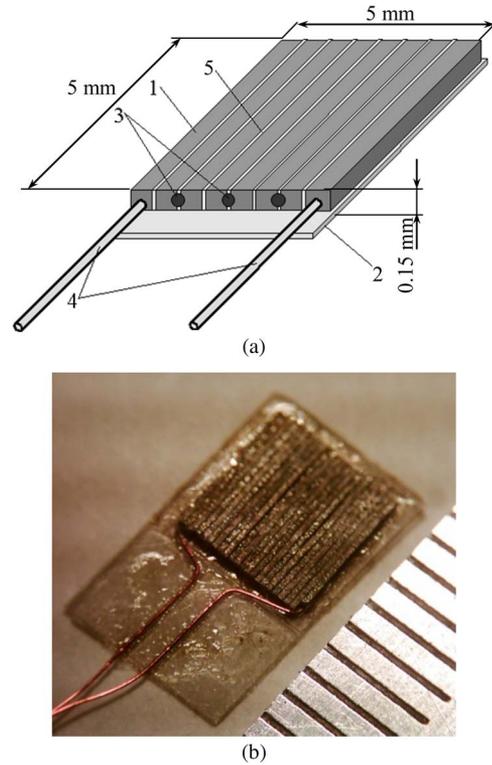

Fig. 3. Gradient heat flux sensor based on bismuth single crystals: (a) 1—bismuth thermoelement, 2—mica base, 3—solderings, 4—wires, 5—insulation, (b) photograph of the GHFS (scale in mm).

However, the heat flux measurement signal is a slowly varying DC component, which can be extracted from the measured signal by an appropriate signal processing unit. In the assembly of the sensor, it is, however, advisable to install the sensor in a direction where the induced AC voltage will be minimized. The connecting wires must also be arranged so that there is a minimum induced AC voltage present. Such an approach makes it easier to find a suitable measuring instrument, which can operate under a significant AC noise signal and a small DC measurement signal. The electrical resistance of a GHFS is about 9 Ω, which provides noise immunity of the measurement circuit. A sensor was tested in a 50 Hz varying flux with an amplitude of 0.7 T. Several millivolts of AC noise signal was induced in the sensor, but simultaneously, a fractional millivolt signal indicating a small heat flux in the air gap was measured without noise. The test was performed by using a Fluke 8840A multimeter.

The response time of the sensor was found from a direct experiment using pulsed laser radiation. The response time of the GHFS is about 10^{-8}–10^{-9} s. It depends only on the design and sensor materials and is independent of their thickness [16].

B. Heat Flux Measurements

Sapozhnikov *et al.* have already used the GHFS for heat flux measurements for a long time [14].

To test the sensors, first, we define the sensitivity. The calibration is described in detail in [15]. The GHFS sensitivity is determined by the absolute method of calibration by using Joule heat. For the sensor, the sensitivity obtained was constant for different heat flux values and different environmental

temperatures. Moreover, during the most recent tests with sensors in the electric power transformer, it is shown that the sensitivity of the sensors is independent of the magnetic field up to 1.2 Tesla. For the GHFS, the combined uncertainty of the volt-watt sensitivity is

$$\Delta S_0 = \sqrt{\left(\frac{\partial S_0}{\partial E}\Delta E\right)^2 + \left(\frac{\partial S_0}{\partial Q}\Delta Q\right)^2}$$

$$= \sqrt{(0,1053 \cdot 0,07 \cdot 10^{-3})^2 + (-1,108 \cdot 10^{-3} \cdot 0,054)^2}$$

$$= 6,04 \cdot 10^{-5} \frac{V}{W} \qquad (2)$$

where E is and Q are the thermo-emf and the heat flux, respectively. The final error of the volt-watt sensitivity is

$$\left(\frac{\Delta S_0}{S_0}\right) \cdot 100\% = \left(\frac{6,04 \cdot 10^{-5}}{9,5 \cdot 10^{-3}}\right) \cdot 100\% = 0,64\%. \quad (3)$$

The second key parameter of any sensor is the response time. The response time was determined by direct calibration. In our experiments, the "hot" surface of the sensor was irradiated by a monochromatic ray for calibration (pulsed laser Nb-YAG, wavelength 635 nm, peak power 50–120 mJ, pulse frequency 1–10 Hz). There is a thermal contact between the "cold" surface of the GHFS and the bulky aluminium plate. The GHFS thermo-emf is processed by a Tektronix TDS3034B oscilloscope. The experiment results show that signal maximum of the GHFS is 10 ns late (concerning the front of a pulse). A decrease in the amplitude was not observed [16].

1) Local Heat Transfer From a Smooth Circular Cylinder in the Cross-Flow of Air: The tests were carried out in a wind tunnel with the following dimensions: diameter 500 mm and air flow up to 30 m/s. The wind tunnel operates in atmospheric conditions. The Reynolds number was varied over the range of $3 \times 10^4 < \text{Re} < 2.5 \times 10^5$. The GHFS was installed flush with the outside surface of the cylinder and connected to the data acquisition system.

The experimental values of the heat transfer coefficient agreed well with the known experimental data. The experimental data gave a value of $\overline{\text{Nu}} = 0.29 \cdot Re^{0.55}$ (compared with the well-known approximation $\overline{\text{Nu}} = 0.22 \cdot Re^{0.6}$[18]). The difference from the equations does not exceed 15%–20%, which is due to various boundary conditions.

2) Natural Convection Close to the Vertical Heated Surface: The object of the study was the natural convection boundary layer formed on the vertical uniformly heated plane surface (height 5 m). A detailed description of the experimental unit is given in [19]. The measurements were made by using a resistance thermometer and a hot wire anemometer.

The root mean square value of the temperature fluctuation and the root mean square value of the heat flux fluctuation that depends on the Grashof number have a good correlation between each other, which shows the reliability of the measurement by a GHFS.

3) Heat Flux Measurement in the Shock Tube [in Cooperation With the Ioffe Institute (St. Petersburg, Russia)]: The experiments were carried out in a gas medium (air and xenon) heated by a strong shock wave with $M = 6 \ldots 10$.
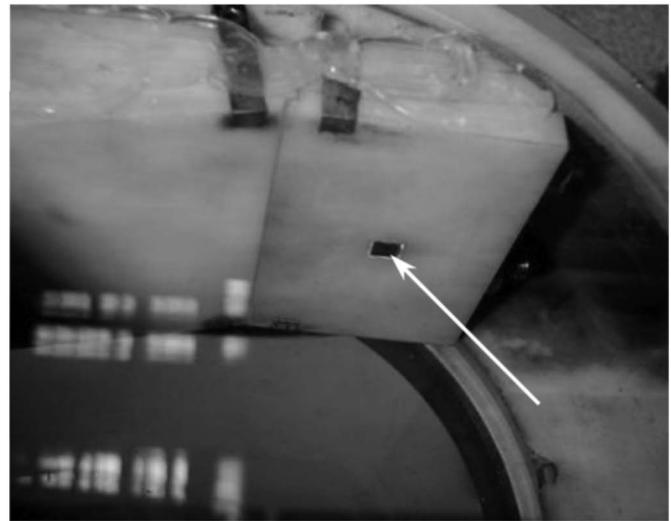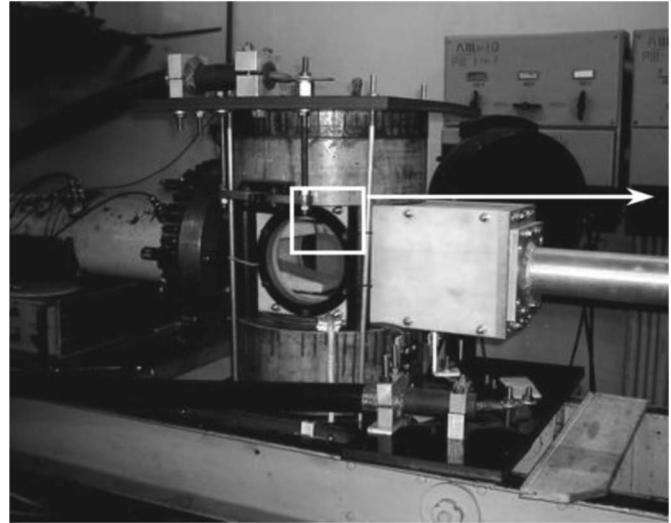

Fig. 4. Sensor in the nozzle.

The experiments were made with a GHFS with an area of 5×5 mm^2 and 0.2 mm thickness pasted on an acrylic plastic (Fig. 4).

The measurement results on a cross section of 100 mm from the closed end are shown in Fig. 5. The pressure transducer pulse (dashed line) abruptly increases at the moments of passing of the incident ($\tau = 0.15$ ms) and reflected ($\tau = 0.55$ ms) shock waves through the recording cross section. The heat flux variation (solid line) completely correlates in time with the pressure transducer signal. The heat flux density in the area after the reflected shock wave (where the gas temperature is $\sim$7000 K) reaches 1.4 MW/m^2. Both the transducers were preliminarily calibrated: the measurement error of the HFS is $\sim$2%, and the pressure transducer 10% at maximum.

Thus, the results showed that the GHFS can be used to measure intensive pulse heat loads related to supersonic and hypersonic gas dynamics. The results of the present study agree well with the heat flux measurements performed with a thin-film resistance element.

4) Heat Transfer in the Mixed and Forced Convection in a Vertical Heated Pipe (in Cooperation With Los-Alamos National Laboratory, USA): The vertical 6 m high heated pipe
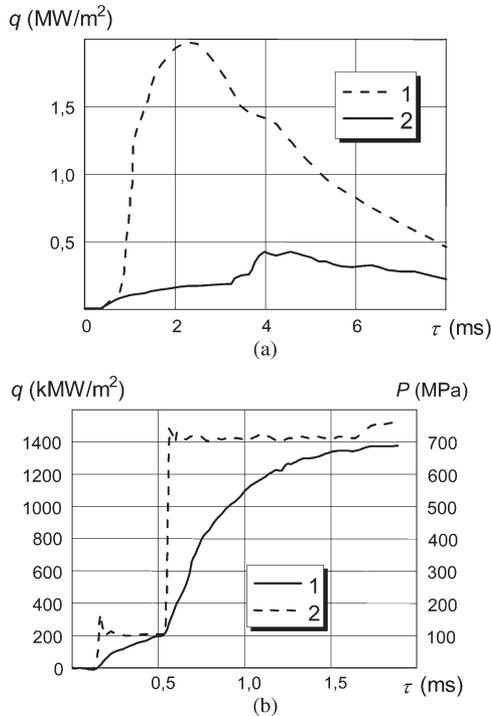
Fig. 5. Experimental results: (a) heat flux (1—sensor in the nozzle; 2—sensor on the tube); (b) heat flux (1) and pressure (2).

TABLE I
MACHINE MAIN PARAMETERS

Number of stator slots, Q_s	12
Number of rotor poles, $2p$	10
Winding factor of the fifth harmonic of the stator (the machine operates at the fifth harmonic), k_{w5}	0.933
Output power, P_{out}	37 kW
Efficiency (with laminated magnets, 20 pieces)	96 %
Speed, n_s	2400 min^{-1}
Line-to-line terminal voltage in star connection, U	400 V
Winding turns in series per stator winding, N_s	64
Rated torque, T_N	147 Nm
Rated current, I_s	60 A
Length of air gap (on both sides of the rotor) δ	2.0 mm
External diameter of the stator stack, $D_{o, axial}$	274 mm
Internal diameter of the stator stack, $D_{i, axial}$	154 mm
Stator yoke height, h_{ys}	21 mm
Thickness of PM, h_{PM}	16 mm
Slot opening width	18 mm
PM remanent flux density, 20 °C, B_{r20C}	1.1 T
PM remanent flux density, 80 °C, B_{r80C}	1.03T
Mass of magnets (NdFeB), m_{PM}	3.9 kg
PM resistivity ρ_{PM}	150 $\mu\Omega cm$
Stator iron material	M270-35A
Permanent magnet material	NEOREM 495a

was the model of the cooling channel for a missile storage facility [17].

The heat transfer in the natural, mixed, and forced convections in a vertical heated pipe was investigated. The tests were performed in two boundary conditions: constant wall temperature and constant heat flux.

The test tube was made of a special steel pipe, the dimensions of which were: diameter 100 mm, length 6 m, and wall thickness 5 mm. The test tube was heated by a direct electrical current through it and by using water heater around the tube. It was possible to change the heated length of the test tube. The test tube was equipped with 11 GHFSs installed inside the tube and 4 outside it (size $5 \times 20 \times 0.3$ mm and sensitivity 10 mV/W).

Heat transfer measurements were performed with varying Grashof and Reynolds numbers. Our results show a good agreement with the theoretical predictions.

III. TEST MACHINE

Present-day neodymium-iron-boron permanent magnets are sensitive to higher temperatures than for example ferrite magnets [1]. Therefore, the heat transfer analysis is important, in particular in permanent magnet machines. Because fractional-slot concentrated-winding synchronous PM machines have been gaining interest over the last few years, also the chosen test machine is a fractional-slot concentrated-winding PM machine [20]–[22]. The prototype PM machine has two stator stacks and one internal, ironless rotor disc, two-layer non-overlapping concentrated tooth windings, and rotor surface magnets. To reduce the large eddy currents induced in the rotor, which in turn cause Joule heating in the rotor, an ironless rotor disc is

used, and sintered rotor-surface permanent magnets are divided into small parts in order to reduce the eddy current losses in the magnets, and further, to enable the use of magnets in certain applications [23]–[26].

The main parameters of the machine are given in Table I [27].

Fig. 6(a) shows one of the stators equipped with a two-layer concentrated winding. Fig. 6(b) illustrates the frame rotor made of fiberglass with magnets inserted.
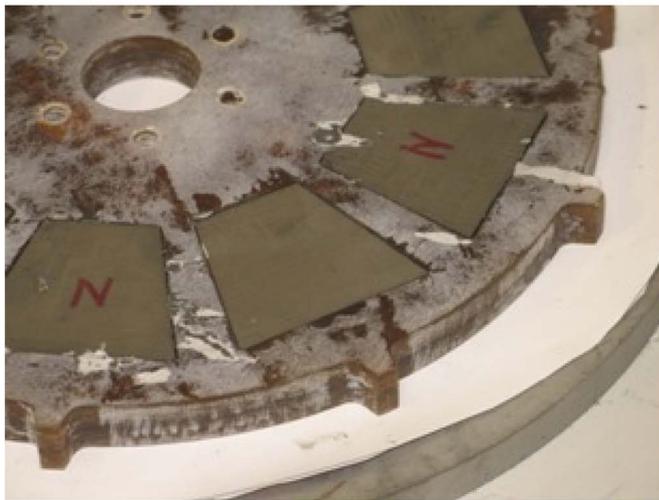
For the heat flux measurement test, one sensor was installed in the stator slot opening area on the glass fiber slot key (Fig. 7). This installation method allows to avoid air bubbles under the sensor; thereby, the final disturbances to the measured heat flux account for about 0.5%, resulting from the thermal resistance of the sensor and its thickness. The sensor thickness is about 0.2 mm, which is less than the viscous sublayer thickness. Thus, the sensor itself does not disturb the air flow. For the installation, high thermal conductivity paste was used. The maybe not-so-obvious place for the sensor was chosen because the air gap between the stator and the rotor is approximately only 2 mm, and the height of the sensor after installation is about 0.5 mm above the metal level. In this paper, the position of the sensor was chosen such that no mechanical work was required with the stator, and mounting of the wires was as simple as possible. If installed on a tooth, where the heat flux is presumably higher, the sensor is likely to be damaged by the rotor during rotation. The point of installation is located lower than this level, and the sensor can be placed there. It is clear that one measuring point is not significant for the total heat flux distribution, but this was only the first test with such a sensor in the heat flux measurement of a PM machine.

Nevertheless, the point of installation is inside the machine having a strong electromagnetic field, and other conditions are equivalent to other parts of the machine in question.

Thus, pilot testing can be carried out to show that GHFSs can be used in permanent machines. In the future tests, a number of sensors will be installed in different points.

(a)

(b)

Fig. 6. (a) One stator equipped with windings. (b) Rotor with magnets assembled.

(a)

(b)

Fig. 7. (a) and (b) Heat flux sensor 10×10 mm^2, installed using thermal paste on the stator slot wedge. The magnetic flux variation will be mostly along the line between the terminals, and therefore, the magnetic-flux-induced AC voltage will come mainly from the sensor connection wires having a clear loop before being twisted. The sensor itself also has some loop surface, in which the AC noise voltage will be induced.
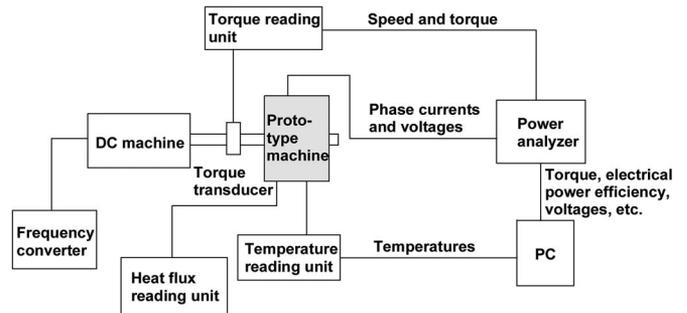
Fig. 8. No-load test arrangement for the concentrated winding axial flux PM.

Fig. 9. Temperatures of windings as a function of time at different rotational speeds.
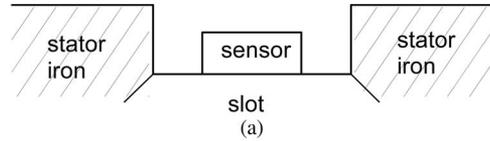
Based on the heat transfer mechanisms, the heat flux vector is always normal to the isotherm lines. Therefore, if the body surface has a constant temperature in a certain area, the heat flux vector (including convection and radiation) is always normal to the surface. Then, applying the conduction mechanism, the heat flux can be transferred into the body in any direction, but always normal to the isotherms.

As the sensor is installed on the surface, it measures the total heat flux, passing through the sensor and coming in or out from the body. The sensor, thereby, cannot measure the heat fluxes inside the body.
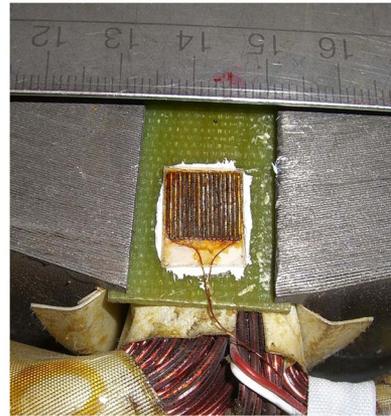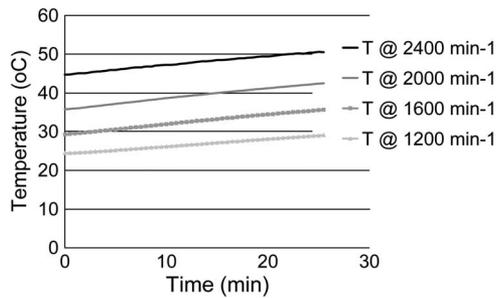
IV. TEST RESULTS

The no-load tests were performed in the generator mode using the DC machine drive as a prime mover. Fig. 8 illustrates the test setup.

The no-load test was performed to evaluate the heat flux in one local point, the induced back-emf of the machine, stator iron losses, the Joule losses of the permanent magnets, and the mechanical loss in no-load conditions. One sensor was used in our pilot tests as described above. At the moment, the measurement is considered sufficiently accurate in one point. The main idea is to test the sensor and the option of using it for on-line heat flux measurement inside permanent magnet machines and similar electric drives.

The stator phase winding temperatures at no load at different rotational speeds from 1200 to 2400 min^{-1} are shown in Fig. 9. Pt100 temperature sensors were used in the phase windings. The temperatures increased during the tests because of the heat

Fig. 10. Temperature has reached 65 °C on the top of a magnet during the measurements.
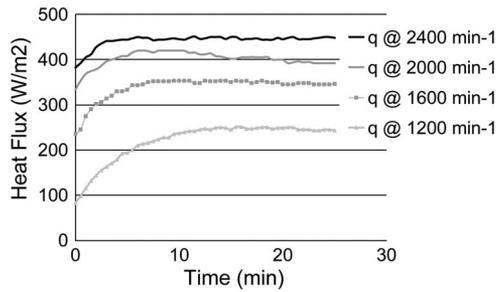

Fig. 11. Heat fluxes in the air gap as a function of time at different rotational speeds. The direction of the heat flux is from the rotor towards the stator slot.

capacity of the machine and did not reach the steady-state condition.

The rotor maximum temperature was measured from top of the magnet using temperature labels. The labels are self-adhesive temperature monitors and consist of heat sensitive indicators sealed under white, heat-resistant windows. The centers of the indicator circle will turn gray at the temperature ratings shown on the label. The color change is irreversible and registers the maximum temperature history of the work piece. The maximum temperature, 65 °C, was achieved at no load with the maximum rotational speed of 2400 min^{-1}, and it is shown in Fig. 10.

The local heat fluxes in the air gap at no load at different rotational speeds varying from 1200 to 2400 min^{-1} are shown in Fig. 11.

At 2400 min^{-1}, the measured no-load losses are 630 W. However, it was not possible to separate the eddy-current contribution that is due to the PMs from the eddy-current contributions that are due to the stator [22], [28]. Finite-element analysis calculations were used to facilitate the definition of the permanent magnet losses and the stator iron losses; the eddy current loss in the magnets was estimated by applying finite element analysis to 110 W, and the measured mechanical losses (air gap friction and bearing losses) were about 170 W [27]. Half of the loss travels in the stator direction, where the HFS is located. The active rotor surface area is about 0.032 m^2, and therefore, the average heat flux at this speed from the magnets
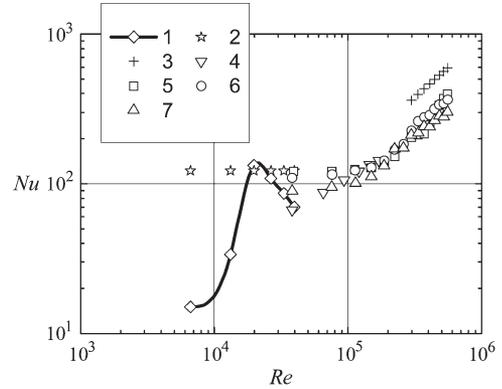

Fig. 12. Local Nu as a function of Re: 1—measured data, 2—laminar flow [12] 3—turbulent free rotor, 4—laminar free rotor, 5—air gap ratio $\delta/r = 0.0106$, 6—$\delta/r = 0.0212$, 7—$\delta/r = 0.0297$ (3, 4, 5, 6, and 7 were taken from [11]. Here, the air gap ratio $\delta/r = 0.0164$, where the air gap $\delta = 2$ mm and the rotor radius $r = 122$ mm.

is about 4.4 kW/m^2. As the teeth are better conducting than the slot areas, the measured heat flux in the range of 450 W/m^2 is within the correct range. The reason for this is that there is no current flowing in the coil during the no-load test. Furthermore, the slot wedges in the stator slots are made of fiberglass, which is a very good insulation material. All the heat is transferred to the teeth, and from there, it is conducted to the copper.

V. COMPARISON OF THE RESULTS

Traditionally, the heat transfer is calculated with the Nusselt number as a function of the Reynolds number (Fig. 12). The Nusselt number is calculated as follows:

$$\text{Nu} = \frac{hr}{k} \tag{4}$$

where h is the heat transfer coefficient (W/(m^{2}K)), r the radius where the sensor is installed (m), and k the air thermal conductivity (0.025 W/(mK)). The Reynolds number is calculated as in [13]

$$\text{Re}_\omega = \frac{\rho \omega r^2}{\mu} = \frac{\omega r^2}{\nu} \tag{5}$$

where ρ(kg/m^3) is the density of the fluid, μ [kg/(ms)] dynamic viscosity of the fluid, ν is the kinematic air viscosity ($1.5 \cdot 10^{-5}$ m^2/s), and ω(s^{-1}) is the rotor speed on the radius r (m). Local heat transfer coefficient is calculated as follows:

$$h = \frac{q}{T_2 - T_1} \tag{6}$$

where q is the heat flux, measured by the sensor (W/m^2), T_2 and T_1 are the temperatures of the stator, measured by the thermopile, and air, far from the motor (20 °C), respectively.

In addition, Fig. 12 shows the local measured Nu from the investigation made by Howey $et\ al.$ [11] and data for laminar flow from [12].

As presented in [12] for the air gap ratio $\delta/r \approx 0.01$ and $2 \cdot 10^4 < \text{Re} < 150 \cdot 10^4$, the local Nu does not depend on Re (curve 2 in Fig. 12). For a disc with $\delta/r < 0.05$, there is a Couette flow between the rotor and the stator. For higher Re, the Nu depends on Re with different ratios.

Our measured data for $6000 < \mathrm{Re} < 20\,000$ are lower than the predicted Nu. This may be explained by the fact that the sensor was installed in a cavity on the fiber insulation plates (see Fig. 7).

For $7000 < \mathrm{Re} < 20\,000$, the local Nu increased from 15 to 150. For $20\,000 < \mathrm{Re} < 40\,000$, the local Nu decreased from 150 to 70, which is practically the same as curve 4 at the same Re. The main difference here compared with [11] is that the Nu number is measured in an actual PM machine, and the sensor is installed in a slot, which represents a down step in the flow. In our further research, we will increase the number of sensors and install them in different points of the stator. Moreover, the target is to record high-speed heat flux pulsation and perform a frequency analysis.

VI. CONCLUSION

The paper describes the application of a local heat flux measurement sensor based on the transverse Seebeck effect in the heat transfer measurement in an AFPM machine. The measurement data were first obtained with the HFS in a PM motor. The sensor measurement results correspond well to the results produced by the heat transfer model of the machine and also to the Nu number analysis reported in different studies in the literature. Direct heat flux measurements can significantly improve the opportunities to evaluate the heat transfer in electrical machines and other heat transfer cases. However, the application of the sensor in different heat transfer cases requires further research with several sensors installed in places that are the most important ones from the heat transfer point of view, and also an in-depth analysis of the fluid flow in the air gap.

The heat flux measurement method offers a significant capability of further developing electrical machines. Sensitive permanent magnets can be protected in a totally new way when exact heat flux components in the machine can be measured. Developing such a method to a level where the measurement results are always reliable makes a breakthrough in the electrical machine development.

REFERENCES

[1] D. A Howey, P. R. N Childs, and A. S Holmes, "Air-gap convection in rotating electrical machines," *IEEE Trans. Ind. Electron.*, vol. 59, no. 3, pp. 1367–1375, Mar. 2012.

[2] J. Nerg, M. Rilla, and J. Pyrhönen, "Thermal analysis of radial-flux electrical machines with a high power density," *IEEE Trans. Ind. Electron.*, vol. 55, no. 10, pp. 3543–3554, Oct. 2008.

[3] D. A. Howey, A. S. Holmes, and K. R. Pullen, "Measurement and CFD prediction of heat transfer in air-cooled disc-type electrical machines," *IEEE Trans. Ind. Appl.*, vol. 47, no. 4, pp. 1716–1723, Jul./Aug. 2011.

[4] "Omega (thin film heat flux sensor, self generating thermopile transducer)," 2012. [Online]. Available: http://www.omega.co.uk/ppt/pptsc.asp?ref=HFS-3_HFS-4&flag=1

[5] D. A. Staton and A. Cavagnino, "Convection heat transfer and flow calculations suitable for electric machines thermal models," *IEEE Trans. Ind. Electron.*, vol. 55, no. 10, pp. 3509–3516, Oct. 2008.

[6] A. Boglietti, A. Cavagnino, and D. Staton, "Determination of critical parameters in electrical machine thermal models," *IEEE Trans. Ind. Appl.*, vol. 44, no. 4, pp. 1150–1159, Jul./Aug. 2008.

[7] T. A. Jankowski, F. C. Prenger, D. D. Hill, S. R. O'Bryan, K. K. Sheth, E. B. Brookbank, D. F. A. Hunt, and Y. A. Orrego, "Development and validation of a thermal model for electric induction motors," *IEEE Trans. Ind. Electron.*, vol. 57, no. 12, pp. 4043–4054, Dec. 2010.

[8] A. Boglietti, A. Cavagnino, D. A. Staton, M. Shanel, M. Mueller, and C. Mejuto, "Evolution and modern approaches for thermal analysis of electric machines," *IEEE Trans. Ind. Electron.*, vol. 56, no. 3, pp. 871–882, Mar. 2009.

[9] F. Sahin and A. J. A. Vandenput, "Thermal modeling and testing of a high-speed axial-flux permanent-magnet machine," *COMPEL, Int. J. Comput. Math. Elect. Electron. Eng.*, vol. 22, no. 4, pp. 982–997, 2003.

[10] D. A. Howey, A. S. Holmes, and K. R. Pullen, "Radially resolved measurement of stator heat transfer in a rotor-stator disc system," *Int. J. Heat Mass Transf.*, vol. 53, no. 1–3, pp. 491–501, Jan. 2010.

[11] D. A. Howey, A. S. Holmes, and K. R. Pullen, "Measurement of stator heat transfer in air-cooled axial flux permanent magnet machines," in *Proc. IEEE Annu. Conf. 35th Ind. Electron.*, Porto, Portugal, Nov. 3–5, 2009, pp. 1197–1202.

[12] S. Harmand, B. Watel, and B. Desmet, "Local convective heat exchanges from a rotor facing a stator," *Int. J. Thermal Sci.*, vol. 39, no. 3, pp. 404–413, Mar. 2000.

[13] C. H. Lim, G. Airoldi, R. G. Dominy, and K. Mahkamov, "Experimental validation of CFD modelling for heat transfer coefficient predictions in axial flux permanent magnet generators," *Int. J. Thermal Sci.*, vol. 50, no. 12, pp. 2451–2463, Dec. 2011.

[14] N. Divin, S. Sapozhnikov, and A. Kirillov, "Gradientenartige Messgeber fur die Messung des Warmestromes," in *Proc. Messtechnik zur Undersuchung von Vorgangen in thermischen Energieanlagen. XXVIII. Kraftwerkstechnisches Kolloquium und 6. Kolloquium Messtechnik fur Energieanlagen*, Dresden, Germany, 1996, pp. 155–160.

[15] S. Z. Sapozhnikov, V. Yu. Mityakov, A. V. Mityakov, A. I. Pokhodun, N. A. Sokolov, and M. S. Matveev, "The calibration of gradient heat flux sensors," *Meas. Tech.*, vol. 54, no. 10, pp. 1155–1159, Jan. 2012.

[16] A. V. Mityakov, S. Z. Sapozhnikov, V. Y. Mityakov, A. A. Snarskii, M. I. Zhenirovsky, and J. J. Pyrhönen, "Gradient heat flux sensors for high temperature environments," *Sens. Actuators A, Phys.*, vol. 176, no. 1, pp. 1–9, Apr. 2012.

[17] M. A. Blinov, M. E. Lebedev, I. S. Muhina, L. A. Feldberg, B. S. Fokin, D. K. Zaitsev, E. L. Kitanin, S. F. Uras, and A. V. Mityakov, "Natural and mixed convection heat transfer of a cooling air in fissile material and spent fuel storage facilities," *Heat Transf. Res.*, vol. 36, no. 4, pp. 295–309, 2005.

[18] A. Zhukauskas, "Heat transfer from tubes in cross flow," in *Advances in Heat Transfer*. New York: Academic, 1972.

[19] A. V. Mitiakov, V. Y. Mitiakov, S. Z. Sapozhnikov, and Y. S. Chumakov, "Application of the transverse seebeck effect to measurement of instantaneous values of a heat flux on a vertical heated surface under conditions of free-convection," *High Temp.*, vol. 40, no. 4, pp. 620–625, Jul. 2002.

[20] A. M. EL-Refaie, "Fractional-slot concentrated-windings synchronous permanent magnet machines: Opportunities and challenges," *IEEE Trans. Ind. Electron.*, vol. 57, no. 1, pp. 107–121, Jan. 2010.

[21] G. De Donato, F. Giulii Gapponi, and F. Caricchi, "No-load performance of axial flux permanent magnet machines mounting magnetic wedges," *IEEE Trans. Ind. Electron.*, vol. 59, no. 10, pp. 3786–3779, Oct. 2012.

[22] R. Di Stefano and F. Marignetti, "Electromagnetic analysis of axial-flux permanent magnet synchronous machines with fractional windings with experimental validation," *IEEE Trans. Ind. Electron.*, vol. 59, no. 6, pp. 2573–2582, Jun. 2012.

[23] H. Polinder and M. J. Hoeijmakers, "Eddy-current losses in the segmented surface-mounted magnets of a PM machine," *IET Elect. Power Appl.*, vol. 146, no. 3, pp. 261–266, May 1999.

[24] H. Toda, Z. Xia, J. Wang, K. Atallah, and D. Howe, "Rotor eddy current loss in permanent magnet brushless machines," *IEEE Trans. Magn.*, vol. 40, no. 4, pp. 2104–2106, Jul. 2004.

[25] W.-Y. Huang, A. Bettayeb, R. Kaczmarek, and J.-C. Vannier, "Optimization of magnet segmentation for reduction of eddy-current losses in permanent magnet synchronous machine," *IEEE Trans. Energy Convers.*, vol. 25, no. 2, pp. 381–387, Jun. 2010.

[26] F. Marighetti and R. Di Stefano, "Electromagnetic analysis of axial flux permanent magnet synchronous machines with fractional windings with experimental validation," *IEEE Trans. Ind. Electron.*, vol. 59, no. 6, pp. 2573–2582, Jun. 2012.

[27] H. Jussila, "Concentrated winding multiphase permanent magnet machine design and electromagnetic properties—Case axial flux machine," Ph.D. dissertation, Acta Universitatis Lappeenrantaensis 374, Lappeenranta Univ. Technol., Lappeenranta, Finland, 2009.

[28] A. Di Gerlando, G. Foglia, M. F. Iacchetti, and R. Perini, "Axial flux PM machines with concentrated armature windings: Design analysis and test validation of wind energy generators," *IEEE Trans. Ind. Electron.*, vol. 58, no. 9, pp. 3795–3805, Sep. 2011.

Hanne K. Jussila was born in Kuusankoski, Finland in 1980. She received the M.Sc. and D.Sc. (Tech) degrees in electrical engineering from the Lappeenranta University of Technology (LUT), Lappeenranta, Finland, in 2005 and 2009, respectively.

Currently, she is a Postdoctoral Researcher and Teacher with the Department of LUT Energy (Electrical Engineering). Her research interests include permanent magnet machines, in particular concentrated winding permanent magnet machines.

Andrey V. Mityakov was born in Leningrad, Russia, in 1974. He received the M.Sc. (Mech.Eng.), Ph.D., and D.Sc. (Tech.) degrees from Leningrad (Saint-Petersburg) State Technical (Polytechnical) University, Saint-Petersburg, Russia, in 1997, 2000, and 2010, respectively.

From 1997 until 2010, he acted as an Associate Professor at the Department of Thermodynamics and Heat Transfer in Saint-Petersburg State Polytechnical University, Saint-Petersburg, Russia. Since 2010, he has been a Professor of the same university. In the year 2011, he started his international work with a position of Professor in Lappeenranta University of Technology (LUT) Institute of Energy Technology at LUT, Finland. His research includes heat transfer (in particular measuring techniques) and data acquisition systems.

Prof. Mityakov is a laureate of the Prize named after the first Rector of Saint-Petersburg Polytechnical Institute, Prince A.G. Gagarin (1998), the medal from the Russian Union of Young Scientists "Devotion to the Science" (2008), winner of the Grant for Young Scientists from the President of the Russian Federation (2008), and Grant for Young Scientists from the Government of Saint-Petersburg (2009).

Sergey Z. Sapozhnikov was born in Lvov, Ukraine, in 1950. He received the Mech.Eng. degree from the Krasnodar Polytechnic Institute, Krasnodar, in 1971, and the and D.Sc.(Tech.) degree from the Ural Polytechnic Institute, Sverdlovsk (now Yekaterinburg), Russia, in 1988.

Currently, he is a Professor at the Department of Thermodynamics and Heat Transfer in Saint-Petersburg State Polytechnical University, Saint-Petersburg, Russia. Prof. Sapozhnikov's research includes material science (bimetals, composites), heat transfer (thermal conductivity particularly), and thermophysical experiment.

Prof. Sapozhnikov is a laureate of the State Committee for High Education Prize (1989); presently, he is a member of the Russian National Committee for Heat Transfer, and a Fellow of the International Power Academy and International Academy of Refrigeration.

Vladimir Y. Mityakov was born in Leningrad, Russia, in 1951. He received the Mech.Eng. and D.Sc. (Tech) degrees at Leningrad Polytechnical Institute (Saint-Petersburg State Polytechnical University), Saint-Petersburg, Russia, in 1970 and 2005, respectively.

Currently, he is a Professor at the Department of Thermodynamics and Heat Transfer in Saint-Petersburg State Polytechnical University, Saint-Petersburg, Russia. His areas of research include heat transfer phenomena in rotating channels.

Juha Pyrhönen (M'06) was born in Kuusankoski, Finland in 1957. He received the D.Sc. (Tech) degree from the Lappeenranta University of Technology (LUT), Lappeenranta, Finland, in 1991.

He became an Associate Professor of Electrical Engineering at LUT in 1993 and a Professor of electrical machines and drives in 1997. Currently, he is the Vice Head of the Department of Electrical Engineering, where he is engaged in the research and development of electric motors and electric drives. His current interests include different synchronous machines and drives, induction motors and drives, and solid-rotor high-speed induction machines and drives.